Convergence of the Adaptive-Wall Wind Tunnel

C. F. Lo* and E. M. Kraft†
ARO, Inc., Arnold Air Force Station, Tenn.

Analytical functional relationships for exterior and interior regions with respect to the control surface inside a two-dimensional wind tunnel are used to investigate the iteration procedure for an adaptive-wall wind tunnel. Convergence to interference-free conditions is proven for any symmetric model in subsonic flow. Also, formulas are presented for determining interference-free conditions directly from two measured flow variables at the measuring plane, thus enabling an adaptive-wall wind tunnel to achieve unconfined flow in a single adjustment. A wavy-wall model and an NACA 0012 airfoil are used as examples to examine the convergence and validate the derivation. In addition, a numerical solution to the transonic small disturbance equation is used to demonstrate the convergence of the adaptive-wall iterative procedure for supercritical flow on an airfoil.

Nomenclature

F = model profile
h = control surface location
k = relaxation factor in physical plane
l = wavelength of wavy-wall model
M = Mach number
p = Fourier transform parameter
S = control surface
u,v = velocity components normalized by freestream velocity in x and y directions, respectively
x,y = streamwise and cross-streamwise coordinates, respectively
β = $\sqrt{1-M^2}$
ϵ = amplitude of wavy-wall model
λ = $2\pi/l$
ϕ = velocity potential normalized by freestream velocity
ω = relaxation factor in transform plane

Subscripts

E = exterior region
T = tunnel interior region
∞ = free-air condition

Superscript

(n) = number of iterations

Notations

$|\ |$ = absolute value
$(\bar{\ })$ = quantity in transform plane

Introduction

LIMITATIONS in transonic test capability have become increasingly evident because of the demand for higher quality data on more sophisticated aerodynamic configurations. In particular, as aircraft models are tested with high-lift transonic wings and at critical maneuvering conditions, the design margins on current aircraft are much closer and therefore require more accurate test data. In recent years, the emphasis in the development of a larger transonic transport (increasing flight Reynolds numbers) has been directed toward a more efficient aircraft with a cruise speed in the transonic range, thus placing even more demands on the quality of the transonic wind tunnel data.

Received May 25, 1977; revision received Sept. 16, 1977.

Index categories: Subsonic Flow; Transonic Flow.

*Supervisor, PWT/4T Analysis Section, AEDC Division. Member AIAA.
†Research Engineer, AEDC Division. Member AIAA.

Of particular concern within the limitations of transonic testing is the effect of the tunnel boundaries. An international ad hoc committee was organized under the auspices of AGARD and a summary of their investigation was given by Monti[1] in 1971. Since then there have been many significant advances[2-4] in the computational schemes to predict wind tunnel boundary interference and in new design concepts to achieve an interference-free tunnel. Additional studies have indicated a need for a spatially variable distribution of porosities and/or plenum pressure.[1,5,6] Consequently, the direction has been taken to develop an adjustable or adaptive wind tunnel wall with a systematic method of eliminating interference.

The use of an adaptive tunnel wall to minimize wall interference is not new.[6-9] However, the early efforts in the development of an adaptive-wall tunnel lacked a methodology for precisely determining the conditions required for interference-free testing. Recently, Ferri and Baronti[10] and Sears[11] independently arrived at an adaptive-wall concept wherein it is recognized that by measuring two flow disturbance quantities and evaluating the requisite functional relationships for unconfined flow, the local wall properties can be systematically adjusted to achieve unconfined flow. An early numerical simulation by Erickson and Nenni[12] established the feasibility of the concept, and recent experimental studies[13-15] have firmly validated the practicality of an adaptive-wall tunnel.

The adaptive-wall concept has been applied innovatively to the numerical solution of unbounded transonic flow in a bounded computational domain by Chen et al.[16] An iterative version of a Dirichlet condition on a matching boundary between a near- and far-field region resulted in convergence of the computations to unbounded flow with a much smaller near field than is normally used in transonic calculations. Under the restrictions of a Dirichlet condition at the matching boundary and a zero initial potential in the far field, a formal proof of convergence of the method was established by functional analysis. By analogy with the adaptive-wall wind tunnel concept, the formal proof in Ref. 16 establishes the convergence of the adaptive-wall concept.

In this paper, analytical simulation of an adaptive-wall tunnel is used to establish conditions for convergence to unconfined flow for subcritical, nonlifting flow in a tunnel with arbitrary initial conditions. By this simulation it then becomes possible to ascertain the rate of convergence and establish criteria to reduce significantly the number of iterations required to achieve unconfined flow. The analysis is performed by using a simplified model of the flow within a tunnel to examine critically the fundamental theoretical validity of the adaptive-wall concept. It should be emphasized that the simulation presented herein differs from the actual process in the following respect. The power of the adaptive-wall concept is that it never requires the calculation of the interior flow (which is presumably complicated, viscous, and probably shock-infested). The wind tunnel acts as an analog device for simulating the complicated flowfield near the model since it is not amenable to computation. Only the flow exterior to the tunnel (presumed to be inviscid, with small disturbances, and weaker shocks, if any) must be determined computationally for the adaptive-wall technique. Hence, in practice, an adaptive-wall tunnel is a "hybrid computer" for accurately solving aerodynamic flowfields by combining the best capabilities of wind tunnel test technology and state-of-the-art computational techniques.

Adaptive-Wall Concept

The basic concept underlying the adaptive-wall wind tunnel, stated in Refs. 10 and 11, say that, to determine whether unconfined flight conditions are obtained in any wind tunnel in the presence of any model configurations, it is necessary and sufficient to determine, for a convenient surface, say S, away from the model and near the walls, whether the measured flow variables at S are consistent with flow in an unconfined region exterior to the tunnel. To make this determination, the distributions of two flow variables (such as velocity components parallel and perpendicular to surface S) are measured at S, and one is used as the boundary value to uniquely specify the flowfield exterior to S in the presence of the condition of unconfined, undisturbed flow of a uniform stream at infinity. Hence, since the two measured distributions constitute redundant boundary data in the presence of the exterior region far-field boundary condition, equality at S of the measured flow variables interior to S and the computed flow variables exterior to S constitutes a definition of interference-free flow in the wind tunnel. Therefore, by comparing the exterior region calculated values with the measured values of the same quantities, it can be determined whether or not unconfined-flow conditions are present in the tunnel.

In general, the process of measurement and calculation just described will reveal that unconfined-flow conditions do not, in fact, prevail in the test section. Unconfined flow conditions could be achieved, however, if provisions are available for adjusting the walls in a logical manner. A basic iterative scheme for modifying the walls to achieve unconfined flow is presented in a block diagram in Fig. 1. First a flowfield is established in the tunnel and the velocity components u_T and v_T (the subscript T indicating measured values in the tunnel) are measured at the given control surface S. The exterior unconfined region is then evaluated by specifying $v_E = v_T$ (subscript E designating the exterior region) as the boundary value at S. If the distribution at S of u_E determined from the exterior region calculation does not agree with u_T, then the flow is still constrained by the walls and the walls must be readjusted. The iteration continues until u_E and u_T agree. Then the flow about the model in the tunnel is unconfined. The relaxation factor k is introduced to accelerate convergence of the iterative process.

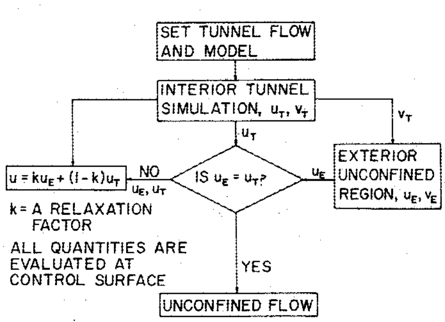

Fig. 1 Iteration procedure for adaptive-wall concept.

The reader should realize that, alternatively, $u_E = u_T$ could be specified at S in the exterior region and v_E compared with v_T to determine if unconfined flow exists in the tunnel. More generally, any two conveniently measurable flow variables can be used in the adaptive-wall process. In addition, the discussion so far is valid for both two- and three-dimensional flowfields.

Analysis

Unconfined Flow Functional Relationships

To provide an analytical proof of convergence of the adaptive-wall concept, a two-dimensional nonlifting model in the subsonic speed range will be used. Consequently, the measuring plane S consists of the parallel planes $y = \pm h$, and because of the symmetry, only the upper region, $y \geq 0$, needs to be examined. The flowfield can be described by the linearized Prandtl-Glauert equation, and the boundary value problem in the exterior unconfined flow region is shown in Fig. 2. If $v_E\,(x,h)$ is the boundary value at $y = h$ along with the condition of unconfined flow at infinity, the boundary-value problem can be solved by the Fourier transform technique. The corresponding unconfined flow distribution $u_E\,(x,h)$ at the measuring plane S is related to the $v_E\,(x,h)$ in the transformed plane as

$$\bar{u}_E(p,h) = (i/\beta)\,(p/|p|)\,\bar{v}_E(p,h) \tag{1}$$

where the barred quantities are the Fourier transformed variables defined by

$$\bar{g}(p,h) = (2\pi)^{-1/2}\int_{-\infty}^{\infty} g(x,h)\,e^{ipx}\mathrm{d}x$$

Alternately, if u_E is the boundary condition at S for the exterior region, then

$$\bar{v}_E(p,h) = -i\beta(p/|p|)\,\bar{u}_E(p,h) \tag{2}$$

Equations (1) and (2) can be inverted into the physical plane as the familiar unconfined-flow functional relationships[11] listed in the Appendix. The unconfined-flow functional relationships of Eqs. (1) and (2) are valid under the Prandtl-Glauert approximation in the exterior region.

Before the analytical simulation of the interior region is presented, the unconfined flowfield is determined about an arbitrary symmetric body located at $y = 0$. By the Fourier transform technique, the streamwise component at the measuring plane $y = h$ in the transformed plane can be written as

$$\bar{u}_\infty(p,h) = (i/\beta)\,(p/|p|)\,\bar{F}(p)\,e^{-\beta h|p|} \tag{3}$$

where

$$\bar{F}(p) = (2\pi)^{-1/2}\int_{-\infty}^{\infty} F_x(x)\,e^{ipx}\mathrm{d}x$$

$F(x)$ is a potential equivalent body shape including viscous effects. The expression for the streamwise component of the velocity in the physical plane is listed in the Appendix.

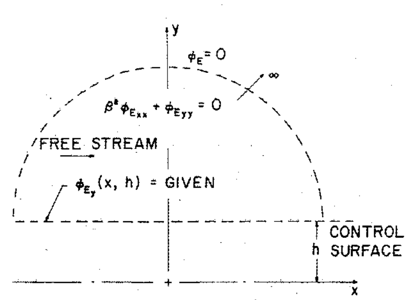

Fig. 2 Boundary-value problem of exterior unconfined region.

The proof of convergence for the adaptive-wall concept thus requires verification that, as the iterative cycle proceeds, the values of the streamwise disturbance velocity at the control surface $y=h$ for both the exterior and interior flowfields become identical and furthermore are equal to the unconfined flow distribution, Eq. (3).

Interior Flowfield Simulation

In order to facilitate the analysis, it is necessary to simulate the interior flowfield mathematically. Again it is emphasized that the great power of the adaptive-wall scheme is that it never requires the calculation of the interior flowfield when applied to a real wind tunnel. The measured tunnel flow is simulated here by the analytical model of the flow in the tunnel described by the boundary-value problem shown in Fig. 3. The same equivalent model geometry is assumed as that in a free-air flow condition. The solution in the interior region is determined in the Fourier-transformed plane if $\bar{v}_T$ (p,h) is specified as

$$\bar{u}_T(p,h) = -\frac{i}{\beta}\bar{v}_T(p,h)\coth(p\beta h) + \frac{i}{\beta}\frac{\bar{F}(p)}{\sinh(p\beta h)} \quad (4)$$

Alternately, if $\bar{u}_T$ (p,h) is specified

$$\bar{v}_T(p,h) = i\beta\bar{u}_T(p,h)\tanh(p\beta h) + \frac{\bar{F}(p)}{\cosh(p\beta h)} \quad (5)$$

Equations (4) and (5) can be inverted to the physical plane as listed in the Appendix.

Convergence of the Iteration Process

The convergence of the iteration procedure will be demonstrated in the transformed plane since the functional relationships are in simple algebraic form in that plane. The iteration is initiated with a given tunnel wall configuration which provides the initial value of flow quantities, $u_T^{(0)}$ and $v_T^{(0)}$, or in the transformed plane, $\bar{u}_T^{(0)}$ and $\bar{v}_T^{(0)}$, at the measuring plane $y=h$. Following the iterative scheme shown in Fig. 1, one can obtain the nth iterative values for $\bar{u}_E$ and $\bar{u}_T$ at $y=h$ by appropriately utilizing Eqs. (1, 2, 4, and 5) to yield

$$\bar{u}_E^{(n)}(p,h) = \begin{cases} -\bar{u}_T^{(0)}(p/|p|)\tanh(p\beta h) + i\Lambda/\beta, n=0 \\ -G_n(p/|p|)\tanh(p\beta h) + i\Lambda/\beta \\ n=1,2,\ldots \end{cases} \quad (6)$$

and

$$\bar{u}_T^{(n)}(p,h) = \omega\bar{u}_E^{(n-1)} + (1-\omega)\bar{u}_T^{(n-1)}$$
$$= G_n, \qquad n=1,2,\ldots \quad (7)$$

where ω is a relaxation factor defined in the transformed plane to accelerate convergence and

$$G_n = G_I\Omega^{n-1} + \frac{i\omega\Lambda}{\beta}\frac{(1-\Omega^{n-1})}{(1-\Omega)}, n=2,3,\ldots \quad (8)$$

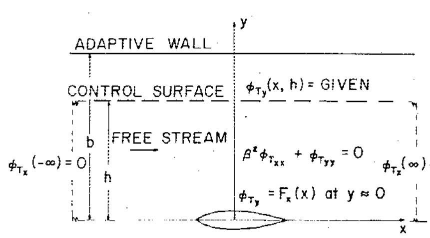

Fig. 3 Boundary-value problem of interior tunnel region.

$$G_I = (i\omega/\beta)(p/|p|)\bar{v}_T^{(0)} + (1-\omega)\bar{u}_T^{(0)} \quad (9)$$

$$\Omega = 1-\omega[1+\tanh(|p|\beta h)] \quad (10)$$

$$\Lambda = (p/|p|)\bar{F}(p)/\cosh(p\beta h) \quad (11)$$

It should be noted that $\Omega^2 < 1$ for $0<\omega<1$. As the iteration proceeds, the effect of the initial tunnel conditions (represented by G_I) diminishes. In the limit as $n\to\infty$ it is readily established that

$$\lim_{n\to\infty} G_n = \frac{i\omega\Lambda}{\beta(1-\Omega)} = \frac{i}{\beta}\frac{p}{|p|}\bar{F}(p)e^{-\beta h|p|} \quad (12)$$

which is equal to $\bar{u}_\infty(p,h)$ as indicated in Eq. (3). Consequently, in the limit $n\to\infty$

$$\lim_{n\to\infty}\bar{u}_E^{(n)}(p,h) = \lim_{n\to\infty}\bar{u}_T^{(n)}(p,h) = \lim_{n\to\infty} G_n = \bar{u}_\infty(p,h) \quad (13)$$

and, hence, convergence of the adaptive-wall method to unconfined flow is established independent of the initial tunnel conditions for nonlifting airfoils in subsonic flow. It is important to note that the iteration procedure converges independently of the relaxation factor for $0<\omega<1$. The significance of the relaxation factor for accelerating convergence will be discussed later on. It should also be noted that convergence can be demonstrated in a similar manner for the alternate procedure of specifying v_T instead of u_T at the control surface.

Simple Example: Wavy-Wall Model

To illustrate further the nature of the iteration process of the adaptive-wall process, a simple wavy-wall model is selected because it was used by Weeks[17] for presumably invalidating the convergence of the adaptive-wall concept. The analysis presented in this section will be used to correct some erroneous conclusions reached by Weeks.‡ The other reason is that the model geometry allows the analysis to be done in the physical plane. The boundary-value problem for a wavy wall in a tunnel is shown in Fig. 4. To start the iteration, any form of the classical linear boundary condition for a tunnel wall is assumed, and the corresponding velocity components at the measuring plane are of the form

$$u_T^{(0)}(x,h) = (\epsilon\lambda/\beta)H_0(h)\sin(\lambda x) \quad (14)$$

$$v_T^{(0)}(x,h) = \epsilon\lambda[-H_0(h)\tanh(\lambda\beta h) + 1/\cosh(\lambda\beta h)]\cos(\lambda x) \quad (15)$$

where $2\pi/\lambda$ is the wavelength of the model, ϵ the amplitude of the waves, and $H_0(h)$ is a function of h and the prescribed tunnel boundary conditions. The nth iterative solution in the physical plane can be obtained as in the previous section as

$$u_E^{(n)}(x,h) = (\epsilon\lambda/\beta)\sin(\lambda x)[-H_n(h)\tanh(\lambda\beta h)$$
$$+ 1/\cosh(\lambda\beta h)], n=0,1,2,\ldots \quad (16)$$

and

$$u_T(n)(x,h) = (\epsilon\lambda/\beta)H_n(h)\sin\lambda x, n=1,2,\ldots \quad (17)$$

where

$$H_n(h) = H_0(h)\kappa^n + k\frac{1}{\cosh(\lambda\beta h)}\frac{1-\kappa^n}{1-\kappa} \quad (18)$$

$$\kappa = 1-k[1+\tanh(\lambda\beta h)] \quad (19)$$

‡Dr. Weeks has recognized and corrected his error.

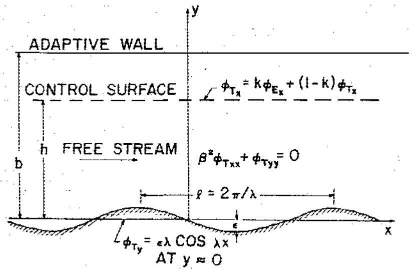

Fig. 4 Wavy wall in a tunnel simulation.

As $n \to \infty$, $H_n(h)$ approaches $k/(1-\kappa)\cosh(\lambda\beta h)$ and

$$\lim_{n\to\infty} u_E^{(n)} = \lim_{n\to\infty} u_T^{(n)} = (\epsilon\lambda/\beta) H_n(h) \sin\lambda x \tag{20}$$

which can be verified to be the unconfined flow solution.

The wavy-wall model also presents an excellent example to examine the acceleration of the convergence by an appropriate selection of the relaxation factor k. Unconfined flow in the tunnel could be accomplished in a single iteration if the boundary could be adjusted to provide

$$H_1(h) = H_0(h)\kappa + k/\cosh\lambda\beta h = e^{-\lambda\beta h} \tag{21}$$

which is equivalent to setting $\kappa = 0$. Hence the optimal relaxation factor is

$$k_{\text{opt}} = \frac{1}{1+\tanh\lambda\beta h} = \frac{1}{2}(1+e^{-\lambda\beta h}) \tag{22}$$

Alternately, if the tunnel wall is adjusted according to a specified $v_T(x,h)$ instead of $u_T(x,h)$, the optimal relaxation factor would be

$$k_{\text{opt}} = \tfrac{1}{2}(1-e^{-\lambda\beta h}) \tag{23}$$

Thus for $\lambda h = 2\pi$ at $M=0.6$, the optimal k are 0.5005 and 0.4995 for specified u_T and v_T, respectively. For these cases and others, Sears[18] has shown that $k=\frac{1}{2}$ is nearly the optimal relaxation factor. These values agree with the value of $k=\frac{1}{2}$ implied in the analysis of Ferri and Baronti[10] to presumably minimize interference in a single wall adjustment.

Weeks[17] employed the same wavy-wall model to question the sufficiency condition of the adaptive-wall concept. By combining flow variables in the interior and exterior regions in various manners, Weeks obtained a pair of mutually derivable independent quantities under the unbounded external flow assumption that did not simultaneously result in interference-free conditions on the model. The fallacy in Weeks' argument is that the two flow variables he derived, in general, could not coexist at the measuring plane in the tunnel.§ Indeed, it can be easily established from Weeks' formulas that his flow variables are functionally compatible only if the tunnel is interference free. As demonstrated in this paper, the iteration procedure converges to unconfined flow.

Historically, and perhaps significantly, Lock and Beavan[8] deduced empirically a weighting factor with a value of 0.6 that is comparable to the acceleration parameter k used in the present analysis. In particular, the procedure used by Lock and Beavan for adjusting their flexible-wall tunnel for a nonlifting airfoil was to position the walls approximately 0.6 of the way between a straight wall and the wall shape for constant pressure. By analogy with the present study, the initial condition in the tunnel corresponds to the straight-wall tunnel which produces $v_T^{(0)}(x,h) = 0$ (allowing for boundary-layer growth). It therefore follows from Eq. (A1) that if $v_E = v_T^{(0)}$, then the external solution is $u_E(x,h) = 0$, which is precisely the requirement for an open-jet (constant pressure) tunnel boundary. Consequently, adjusting the tunnel boundary to produce a constant pressure boundary is an empirical method for determining the external solution $u_E(x,h)$. And indeed, an appropriate weighting of the internal and external solutions can produce the conditions for unconfined flow. In the next section, a technique for producing interference-free conditions in a single-step iteration will be examined.

§Weeks' fallacy has been indicated independently in a similar manner by W. R. Sears of the University of Arizona.[19]

Single-Step Convergence to Unconfined Flow

A technique for determining conditions for unconfined flow in a single step is of paramount importance. Only a single wall adjustment would be necessary for an adaptive-wall wind tunnel, thus significantly reducing tunnel time. For a nonlifting airfoil in subcritical flow, the conditions for unconfined flow in a tunnel can be determined by choosing an optimal relaxation factor in Eq. (7).

The optimal relaxation factor ω can be obtained by setting $\Omega = 0$ in Eq. (10) as

$$\omega_{\text{opt}} = 1/[1+\tanh(|p|\beta h)] \tag{24}$$

which is in the transformed plane and can be used to reduce the iterative procedure to a single step. By substituting ω_{opt} of Eq. (24) into Eq. (7), one obtains the streamwise velocity component in the transformed plane

$$\bar{u}_T^{(1)}(p,h) = [\bar{u}_E^{(0)}(p,h)\cosh p\beta h + \bar{u}_T^{(0)}(p,h) \times \sinh|p|\beta h] e^{-|p|\beta h} \equiv \bar{u}_\infty(p,h) \tag{25}$$

which can be inverted to yield in the physical plane

$$u_\infty(x,h) = \tfrac{1}{2}[u_E^{(0)}(x,h) + u_T^{(0)}(x,h)] + \frac{1}{2\pi}\int_{-\infty}^{\infty} \frac{u_E^{(0)}(\xi,h) - u_T^{(0)}(\xi,h)}{(x-\xi)^2 + (2\beta h)^2} d\xi \tag{26}$$

Therefore, with a single calculation of the external region, unconfined flow conditions can be specified at the measuring plane. It is interesting to note that the first term of Eq. (26) is equivalent to the result that specifying the relaxation factor to be ½ in the physical plane would produce. Hence the second term of Eq. (26) indicates the amount of error produced if the method of Ferri and Baronti[10] were used. In addition, it is indicated by Eq. (26) that a simple linear algebraic combination of u_E and u_T will not produce interference-free conditions in a single iteration.

The conditions for unconfined flow at the measuring plane can also be written directly in terms of the quantities $u_T(x,h)$ and $v_T(x,h)$ measured near the tunnel boundaries by using Eqs. (1) and (25):

$$u_\infty(x,h) = \frac{1}{2}u_T(x,h) - \frac{\beta h}{\pi}\int_{-\infty}^{\infty} \frac{u_T(\xi,h)}{(2\beta h)^2 + (\xi - x)^2} d\xi - \frac{1}{2\pi\beta}\oint_{-\infty}^{\infty} \frac{v_T(\xi,h)}{(\xi - x)} d\xi - \frac{1}{2\pi\beta}\int_{-\infty}^{\infty} \frac{v_T(\xi,h)\cdot(\xi - x)}{(2\beta h)^2 + (\xi - x)^2} d\xi \tag{27}$$

Similarly, the normal component of velocity is

$$v_\infty(x,h) = \frac{\beta}{2\pi}\oint_{-\infty}^{\infty} \frac{u_T(\xi,h)}{(\xi - x)} d\xi - \frac{\beta}{2\pi}\int_{-\infty}^{\infty} \frac{u_T(\xi,h)\cdot(\xi - x)}{(2\beta h)^2 + (\xi - x)^2} d\xi + \frac{1}{2}v_T(x,h) + \frac{\beta h}{\pi}\int_{-\infty}^{\infty} \frac{v_T(\xi,h)}{(2\beta h)^2 + (\xi - x)^2} d\xi \tag{28}$$

Equations (27) and (28) demonstrate that the measurement of the *two* flow variables at the measuring plane $y=h$ is

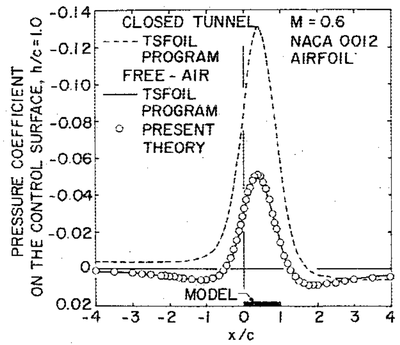

a) **Pressure coefficient**

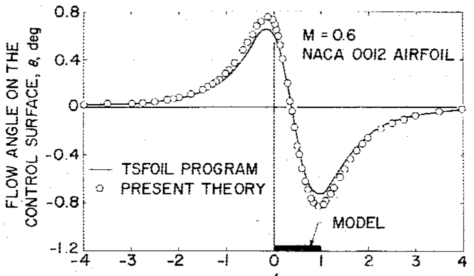

b) **Flow angle**

Fig. 5 Numerical demonstration of single-step iteration to unconfined flow at the control surface for airfoil at zero incidence.

necessary and sufficient to determine the unconfined-flow conditions at the tunnel boundaries. Another application of Eqs. (27) and (28) is to solve the interference flowfield by specifying the difference of velocity components between measured tunnel and free-air conditions at the measuring plane. The interference velocity components are obtained[20] solely in terms of the two measured variables at $y=h$. Hence, for the conventional wall tunnel, the interference can be assessed without modeling the test article or assuming some characteristic for the wall as in classical wall interference theory.

Numerical Demonstration

Subsonic Flow Condition

To validate the method introduced in the previous sections, numerical experiments were performed simulating the flow in a wind tunnel with the inviscid, transonic small disturbance equation. In the first demonstration, the transonic airfoil program TSFOIL[21] developed by Murman and his coworkers was used to simulate the flow past an NACA 0012 airfoil at $M=0.6$ in a tunnel with a solid boundary at $h/c=1.0$. The distributions $u_T\ (x,h)$ and $v_T\ (x,h)$ [$v_T\ (x,h)=0$ for the solid boundary] were substituted into Eqs. (27) and (28) to determine the flow variables required for unconfined flow at the tunnel boundary. The results from Eqs. (27) and (28) are compared in Fig. 5 with the closed-wall flow variables and the flow variables at $h/c=1.0$ determined from the TSFOIL program for the airfoil at zero incidence in unconfined flow. Numerical computation of Eqs. (27) and (28) is treated by removing the singularity of the Cauchy integrals and using a simple numerical quadrature integration. Indeed, a good approximation to the required flow variables for unconfined flow can be determined directly from the measured variables $u_T\ (x,h)$ and $v_T\ (x,h)$. Consequently, for a nonlifting airfoil in subcritical flow, the information is available to attain unconfined flow in a single adjustment of an adaptive wind tunnel wall.

Fig. 6 Pressure distribution for several iterative steps for supercritical flow, $M=0.90$, $\alpha=0$, $k=0.5$.

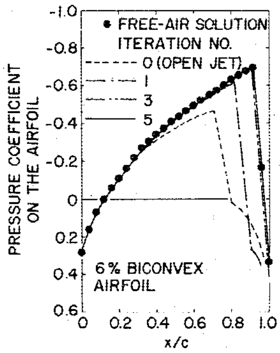

Transonic Flow Condition

The theory presented in this paper is formally valid only for nonlifting airfoils in subcritical flow. However, the primary use for the adaptive-wall method is in transonic testing, where local supercritical velocities are present. Thus, to demonstrate the effectiveness of the adaptive-wall method even for supercritical flow, a numerical simulation of the interior and exterior regions was performed using a Murman et al.[21] type solution to the transonic small disturbance equation. A typical result for a 6% biconvex airfoil at $M=0.9$ in a tunnel with an initial open-jet boundary ($u_T\ (x,h/c=1)=0$) is shown in Fig. 6. Since Eqs. (27) and (28) are no longer valid, a relaxation factor, $k=0.5$, was used to accelerate the convergence of the scheme. For the example shown in Fig. 6, the supercritical region and shock wave extend beyond the measuring plane at $h/c=1$. Even for this supercritical case, excellent results are achieved in three iterations and complete convergence to unconfined-flow conditions was obtained in five iterations.

Concluding Remarks

Application of an analytical simulation of the subcritical flow past a nonlifting airfoil in a wind tunnel test section has shown that the adaptive-wall wind tunnel scheme converges to the unconfined-flow conditions regardless of the initial conditions at the tunnel boundaries. Furthermore, for a nonlifting airfoil, a set of functional relationships has been derived for determining the conditions at the tunnel boundary required for unconfined flow directly from the flow variables measured near the wall. Consequently, for an adaptive-wall wind tunnel, it is conceivable that unconfined flow could be attained in a single adjustment of the tunnel boundary. It therefore appears essential that the ideas contained in this paper should be extended to the lifting case and to three-dimensional flowfields to enhance the practicality of an adaptive-wall wind tunnel.

Appendix

The functional relationships in the unconfined flow at the measuring plane $y=h$ are

$$u_E(x,h) = \frac{-1}{\pi\beta} \fint_{-\infty}^{\infty} \frac{v_E(\xi,h)}{\xi - x} \mathrm{d}\xi \tag{A1}$$

and

$$v_E(x,h) = \frac{\beta}{\pi} \fint_{-\infty}^{\infty} \frac{u_E(\xi,h)}{\xi - x} \mathrm{d}\xi \tag{A2}$$

The streamwise component of the unconfined flow about a symmetric body at the measuring plane $y=h$ is

$$u_\infty(x,h) = \frac{-1}{\pi\beta} \int_{-\infty}^{\infty} \frac{F_\xi(\xi)(\xi - x)}{(\xi - x)^2 + (\beta h)^2} \mathrm{d}\xi \tag{A3}$$

The functional relationships in the interior region at the measuring plane $y = h$ are

$$u_T(x,h) = \frac{1}{2\pi\beta^2}\int_{-\infty}^{\infty} v_T(\xi,h)\coth\frac{\pi(\xi - x)}{2\beta h}\,d\xi + \frac{1}{2\pi\beta^2}\int_{-\infty}^{\infty} F_\xi(\xi)\tanh\frac{\pi|\xi - x|}{2\beta h}\,d\xi \quad (A4)$$

$$v_T(x,h) = \frac{-1}{2h}\int_{-\infty}^{\infty} u_T(\xi,h)\Big/\sinh\frac{\pi(\xi - x)}{2\beta h}\,d\xi + \frac{1}{2\beta h}\int_{-\infty}^{\infty} F_\xi(\xi)\Big/\cosh\frac{\pi(\xi - x)}{2\beta h}\,d\xi \quad (A5)$$

Acknowledgment

The research reported herein was performed by the Arnold Engineering Development Center, Air Force Systems Command. Work and analysis for this research was done by personnel of ARO, Inc., a Sverdrup Corporation Company, operating contractor of AEDC. Further reproduction is authorized to satisfy needs of the U.S. Government. The contribution of W. L. Sickles on the numerical computation of subsonic flow case is greatly appreciated.

References

[1] Monti, R., "Wall Corrections for Airplanes with Lift in Transonic Wind Tunnel Tests," Part II, AGARD AR-36-71, Aug. 1976.

[2] "Wind Tunnel Design and Testing Techniques," AGARD-Conference Proceedings No. 174, Oct. 1975.

[3] *AIAA 9th Aerodynamic Testing Conference Proceedings*, Arlington, Texas, June 1976.

[4] Kraft, E. M. and Lo, C. F., "Analytical Methods for Determining Biockage Effects in a Perforated-Wall Transonic Wind Tunnel," *AIAA Journal*, Vol. 15, April 1977, pp. 511-517.

[5] Lo, C. F., "Wind Tunnel Wall Interference Reduction by Streamwise Porosity Distributions," *AIAA Journal*, Vol. 10, April 1972, pp. 547-550.

[6] Kraft, E. M., "An Integral Equation Method for Boundary Interference in Perforated-Wall Wind Tunnels at Transonic Speeds," Ph.D. Dissertation, University of Tennessee, December 1975; also published as AEDC-TR-76-43, April 1976.

[7] Preston, J. H. and Sweeting, N. E., "Experimental Determination of the Interference on a Large Chord Symmetrical Joukowski Aerofoil Spanning a Closed Tunnel," ARC R&M 1977, 1942.

[8] Lock, C. N. H. and Beavan, J. A., "Tunnel Interference at Compressibility Speeds Using the Flexible Walls of the Rectangular High-Speed Tunnel," ARC R&M 2005, 1944.

[9] Preston, J. H., Sweeting, N. E., and Cox, D. K., "The Experimental Determination of the Two-Dimensional Interference on a Large Chord Piercy 12/40 Aerofoil in a Closed Tunnel Fitted with a Flexible Roof and Floor," ARC R&M 2007, 1944.

[10] Ferri, A. and Baronti, P., "A Method for Transonic Wind Tunnel Corrections," *AIAA Journal*, Vol. 11, Jan. 1973, pp. 63-66.

[11] Sears, W. R., "Self-Correcting Wind Tunnels," Calspan Report No. RK-5070-A-2, July 1973; also the *Aeronautical Journal*, Vol. 78, No. 758/759, Feb./March 1975, pp. 80-89.

[12] Erickson, J. C. Jr. and Nenni, J. P., "A Numerical Demonstration of the Establishment of Unconfined-Flow Conditions in a Self-Correcting Wind Tunnel," Calspan Report RK-5070-A-1, Nov. 1973.

[13] Vidal, R. J., Erickson, J. C. Jr., and Catlin, P. A., "Experiments with a Self-Correcting Wind Tunnel," *AGARD Conference Proceedings No. 174 on Wind Tunnel Design and Testing Techniques*, Paper No. 11, Oct. 1975.

[14] Chevallier, J. P., "Soufflerie Transsonique a Porois Auto-Adaptables," *AGARD Conference Proceedings No. 174 on Wind Tunnel Design and Testing Techniques*, Paper No. 12, Oct. 1975.

[15] Goodyer, M. J., "A Low Speed Self Streamlining Wind Tunnel," *AGARD Conference Proceedings No. 174 on Wind Tunnel Design and Testing Techniques*, Paper No. 13, Oct. 1975.

[16] Chen, A. W., Dickson, L. J., and Rubbert, P. E., "A Far Field Matching Method for Transonic Computations," AIAA Paper 77-208, AIAA 15th Aerospace Sciences Meeting, Jan. 1977.

[17] Weeks, T. M., "Reduction of Transonic Slotted Wall Interference by Means of Slat Contouring," AFFDL-TR-74-139, March 1975.

[18] Sears, W. R., "A Note on Adaptive-Wall Wind Tunnels," April 1976 (unpublished paper).

[19] Sears, W. R., private communication, Oct. 1975.

[20] Lo, C. F., "Tunnel Interference Assessment by Wall Measurements" (to be submitted to *AIAA Journal*).

[21] Murman, E. M., Bailey, F. R., and Johnson, M. L., "TSFOIL—A Computer Code for Two-Dimensional Transonic Calculations, Including Wind-Tunnel Wall Effects and Wave-Drag Evaluation," NASA SP-347, March 1975, pp. 769-788.